LBL-38518
UC-410
CONF-9509134--2

# Lawrence Berkeley Laboratory

UNIVERSITY OF CALIFORNIA

## Accelerator & Fusion Research Division

Presented at the Second International Symposium on Metallic Multilayers, Cambridge, United Kingdom, September 11–14, 1995, and to be published in the Proceedings



**Status and Limitations of Multilayer X-Ray Interference Structures**

J.B. Kortright

March 1996



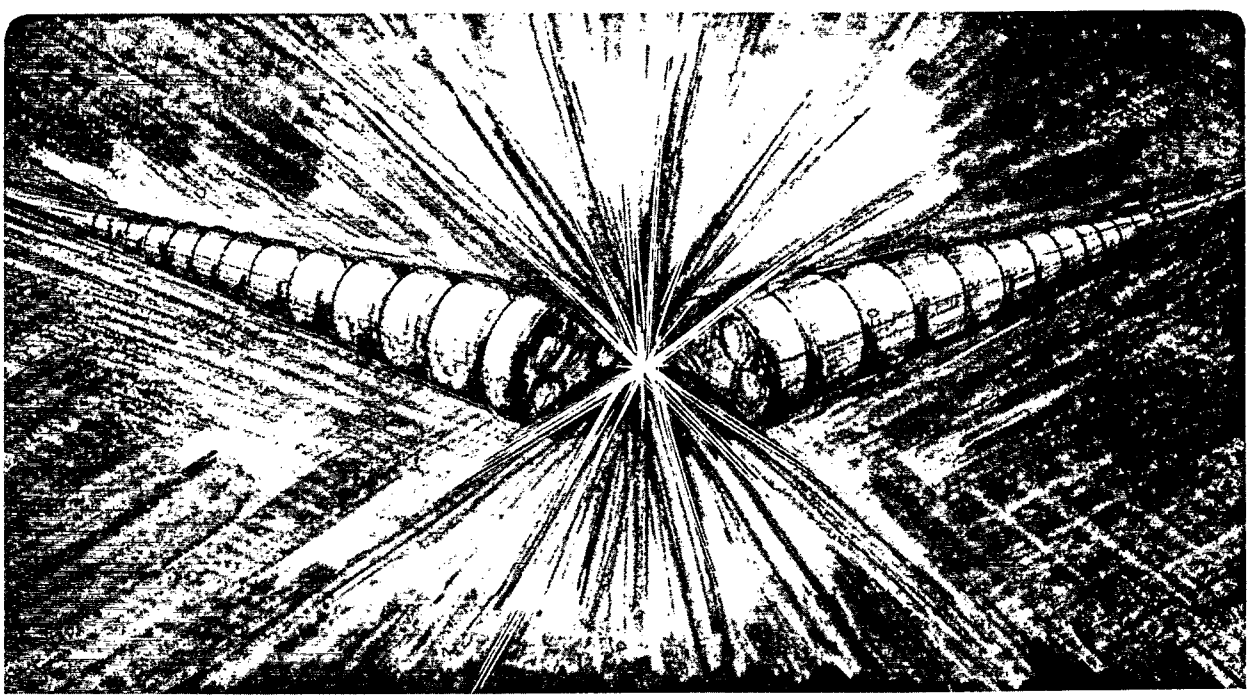

**Prepared for the U.S. Department of Energy under Contract Number DE-AC03-76SF00098**

LBL-38518
LSBL-319
UC-410

# STATUS AND LIMITATIONS OF MULTILAYER X-RAY INTERFERENCE STRUCTURES*

J.B. Kortright

Center for X-Ray Optics
Advanced Light Source
Lawrence Berkeley National Laboratory
University of California
Berkeley, California 94720

*This work was supported by the Director, Office of Energy Research, Office of Basic Energy Sciences, Materials Sciences Division, of the U.S. Department of Energy, under Contract No. DE-AC03-76SF00098.

*presented at 2nd International Symposium on Metallic Multilayers*
*Cambridge, UK, 11-14 September 1995*
*to appear in proceedings, JMMM*



# Status and Limitations of Multilayer X-Ray Interference Structures

J.B. Kortright
Center for X-Ray Optics and Advanced Light Source
Lawrence Berkeley National Laboratory
Berkeley, California 94720 USA

*Version 2, 28 September 1995*

Trends in the performance of x-ray multilayer interference structures with periods ranging from 9 to 130 Å are reviewed. Analysis of near-normal incidence reflectance data vs. photon energy reveals that the effective interface width σ in a static Debye-Waller model, describing interdiffusion and roughness, decreases as the multilayer period decreases, and reaches a lower limit of roughly 2 Å. Specular reflectance and diffuse scattering from uncoated and multilayer-coated substrates having different roughness suggest that this lower limit results largely from substrate roughness. The increase in interface width with period thus results from increasing roughness or interdiffusion as the layer thickness increases.

Keywords: multilayer, x-ray reflectance, x-ray scattering, roughness

In the past 15 years, the study of multilayer x-ray interference structures has evolved from first demonstration experiments, through much study as novel nanoscale structures, to a point where their structures and limitations to performance are becoming understood. Applications of x-ray multilayers can be grouped into three categories based on the incident angle range of use; near-normal incidence (20 - 350 eV), polarizing near 45° (35 - 900 eV), and grazing incidence (50 - 50,000 eV). The high energy limit for these applications is set by the scattering vectors $q = 4\pi\sin\theta/\lambda = 2\pi/d$ available from multilayers having period d as small as 9 Å and by the effects of imperfections, which increase with q. This paper summarizes the status of multilayer x-ray interference structures, with emphasis on understanding the limits to their optical performance. Normal incidence reflectance performance is reviewed, with analysis that provides insight into the nature of limiting imperfections. Specular reflectance and diffuse scattering data demonstrate that substrate roughness becomes a dominant limitation reached by high quality, small period multilayers.

Multilayer x-ray interference structures comprise periodic or quasi-periodic arrangements of alternating layers of two materials whose bi-layer thickness, or period d, is designed to position a constructive interference at the Bragg condition $\lambda = 2d\sin\theta$ relating d, wavelength $\lambda$, and grazing incidence angle $\theta$. Their optical properties are equivalently described as extensions of longer wavelength (visible, UV) optical interference in multilayer thin films [1,2], or as short wavelength (x-ray) Bragg diffraction in crystals [2,3]. Both optical and material properties influence the choice of materials for inclusion in x-ray multilayers. Using the complex refractive index $n(\lambda) = 1 - \delta(\lambda) - i\beta(\lambda)$, material pairs which optimize reflectance have optical constants $\delta$ and $\beta$ well-separated in the $\delta$-$\beta$ plane and limited overall absorption ($\beta$) to increase the number of layers contributing to the interference [4,5]. Material pairs typically selected contain a weak scatterer near the origin in the $\delta$-$\beta$ plane, and a strong scatterer far from the origin. Consideration of materials properties typically rules out low melting point and highly reactive materials, favoring refractory materials. Commonly used strong scattering materials include W, Mo, Ru, Rh, Pd, Ge, Ni, Co, Fe, and Cr. Commonly used weak scattering materials include C, Si, B, Al, Be, Sc, Ti, $B_4C$, BN, and SiC. The optical criteria generally select materials that are well-separated in the periodic table and that do not share a common crystal structure, so that heteroepitaxy is generally not desired. Useful structures

are grown by several techniques, including electron beam evaporation [6], magnetron sputtering [7], ion beam deposition, laser beam deposition, and electron cyclotron resonance sputtering. Magnetron sputtering is most frequently used, and produces structures whose reflectance is unsurpassed by those grown using other techniques. Materials interactions at the interfaces influence the interatomic structure of multilayers and hence their microstructural perfection. The multilayers discussed below are high quality in that deposition kinetics and thermodynamics result in well-defined, continuous layers which possess useful x-ray interference properties approaching those of the ideal structures after which they were designed.

Several structural imperfections can degrade the optical properties of real x-ray multilayers. An ideal multilayer would have atomically abrupt chemical gradients across the interfaces (along z) and perfectly flat, smooth interfaces (in x-y plane) over all spatial frequencies. Unwanted overlayers only nanometers thick can degrade reflectance, especially below several hundred eV where $\delta$ and $\beta$ can be large enough to be a significant optical perturbation. Interdiffusion across interfaces reduces reflectance by reducing the composition modulation. Interface roughness reduces specular reflectance by scattering into non-specular directions [8,9]. Reduced performance can also result from systematic or random errors in multilayer deposition, including unwanted layer thickness variation, chemical contamination of layers, and substrate temperature variation.

Distinguishing between interfacial roughness and interdiffusion is possible in principle through careful study of specular reflectance and non-specular scattering. Both roughness and interdiffusion reduce specular reflectivity, and a static Debye-Waller factor, $\exp[-(\sigma q)^2]$, is often used to model reduced reflectance at each interface to simulate these effects. Here $\sigma$ represents an interface width that may contain contributions from each effect and may be different for different interfaces. This static Debye-Waller factor reduces the peak intensity of multilayer Bragg peaks but has little effect on peak width. Diffuse (non-specular) scattering results only from roughness, an so can help establish the specific contribution of roughness. Several theoretical models describe the effects of roughness on scattering in multilayers [10-13]. Interdiffusion, if limited to small intermixing at the interfaces, can be described by this static Debye-Waller term [14], and thus can reduce peak intensity without significantly affecting peak width. However, interdiffusion and reaction can proceed much more extensively, forming distinct interface

layers of specific composition (as in Mo/Si multilayers [15-16]), or even completely transforming the composition of one layer (typically the strong scatterer) to one similar to an intermetallic compound of the constituents. This strong interdiffusion can, but does not necessarily, significantly alter the optical contrast of the two layers. Reduced optical contrast due to interdiffusion or chemically mixed layers not only reduces peak reflectance, but also results in observable peak narrowing [17,18].

Recently a survey was conducted within the x-ray multilayer community in which numerous groups reported on the measured reflectance of multilayers they had grown specifically as x-ray reflectors [19]. The survey results concerning near normal incidence reflectance are shown in Fig. 1a, which plots peak reflectance measured near 85° incidence angle as a function of hν. Maximum peak reflectance occurs near 110 eV. For some time Mo/Si multilayers had the highest reflectance (about 0.64) just below the Si $L_{2,3}$ edge at 99.5 eV, and recently Mo/Be has yielded 0.68 just below the Be K edge at 111.5 eV [20]. Below 95 eV reflectance decreases. Here $\delta$ and $\beta$ are increasing, so that even thin contamination layers can significantly degrade reflectance [21]. Below roughly 20 eV all materials are so strongly absorbing that multilayers have periods thicker than an absorption length, so that significant multilayer interference can not occur. Above 110 eV peak reflectance decreases rapidly from 0.68 to roughly 0.06 at 280 eV, resulting in part from the changing optical properties of materials and in part from the increasingly important effects of structural imperfections as q increases.

Comparing measured peak reflectance with calculated values provides some insight into the interface imperfections which limit performance. Figure 1b shows the ratio of measured peak reflectance to that calculated for ideal structures corresponding to those samples in Fig. 1a exhibiting the best reflectance with hν. Calculations are based on published values of optical constants [22] and assume chemically pure layers with bulk densities. The decrease in this ratio above 100 eV is easily understood from the Debye-Waller factor $\exp[-(\sigma q)^2]$, since $q \propto h\nu$. Assuming $\sigma$ is constant for all of the multilayers in Fig. 1a, the ratio of the measured to ideal peak reflectance is expected to decrease with increasing hν, as observed. However, further analysis of these data reveal that $\sigma$ is not constant for these multilayers, but varies in a specific manner. Assuming that the Debye-Waller factor alone describes roughness and interdiffusion effects, calculations were made in which $\sigma$ was varied to match calculated and measured

peak reflectance. Resulting σ values are plotted vs. d in Fig. 2. Data in Fig. 2 have been extended to lower d than allowed by the normal incidence survey results by including σ values from $W/B_4C$ multilayers with 9 Å < d < 40 Å as obtained from an identical analysis of grazing incidence Cu $K_\alpha$ reflectance measurements (solid triangles). A trend of decreasing σ with d is apparent, and remarkable in that multilayers composed of a broad range of materials with widely different periods all yield values which scatter along the line shown. If σ alone is used to gauge perfection, then high quality x-ray multilayers become more perfect as their period decreases. Even so, $\sigma q = 2\pi\sigma/d$ increases as d decreases, accounting for the reduced ratio of measured to calculated ideal reflectance as d decreases. It is tempting to conclude that roughness increases as d increases. For some of the multilayers in the survey sample, notably the immiscible Ru/C samples, this appears to be the case. For reactive systems interdiffusion also contributes to the reduced measured reflectance. Regardless of this distinction, the data indicate a lower limit to σ of approximately 2 Å.

The origin of this lower limit to the interface width σ is of interest. We can distinguish between intrinsic structural imperfections originating within multilayers (roughness, interdiffusion) and extrinsic imperfections (substrate roughness, unwanted overlayers). The above analysis implies, since σ increases with d, that a growing contribution to σ results from intrinsic effects as d increases. The limiting value of σ at small d is inferred to result at least partly from extrinsic effects, in particular substrate roughness.

We have investigated the effects of substrate roughness by measuring specular x-ray reflectivity and non-specular x-ray scattering from a set of fused silica substrates polished to 4 different levels of smoothness, and from W/C multilayers (d = 30.6 Å, N = 40) deposited simultaneously on an identical set of 4 substrates. The smoothest substrate is typical of the best polished substrates available for x-ray mirrors. Measurements were made using 1.38 Å synchrotron radiation, and will be reported elsewhere in detail. Figure 3a shows the true specular reflectance (diffuse scattering subtracted) of the 4 different substrates, along with fits to the data points yielding σ values ranging from 2.2 Å to 19.1 Å. Figure 3b shows a specular scan from the W/C multilayer on the smoothest substrate, along with an offset scan measuring diffuse intensity nominally parallel to the specular scan but offset by $q_x \cong 0.002$ Å$^{-1}$ in the plane of the layers. A σ = 2.7 Å is needed to match calculated and measured 1st order multilayer peak

reflectance. Microstructural characterization of the W/C system reveals intermixing of W and C at the interfaces and diffusion of C into the amorphous W-rich layers [23,24], which can account for the increase in the multilayer $\sigma$ above that of the substrate. The offset scan shows diffuse Bragg peaks which are just as intense, relative to the background between the peaks, as the specular Bragg peaks, indicating that the roughness yielding this diffuse intensity has identical vertical (z) correlations as the multilayer itself. This is not surprising, considering the low value of the in-plane spatial frequency, $q_x$, at which the offset scan was made. It would be surprising if multilayer roughness were not highly vertically correlated at in-plane wavelengths of $2\pi/q_x \cong 3000$ Å. Non-specular scattering studies with the scattering plane normal to the multilayer surface generally sample in-plane frequencies much lower than the multilayer fundamental [9].

Transverse rocking scans probe more directly the in-plane height or roughness correlations in the different substrates and multilayers. Rocking scans with identical trajectories in q-space for the uncoated substrates and multilayer-coated substrates are in Fig. 4 (a) and (b), respectively. In-plane height correlations are very different for the 4 substrates. Likewise, in-plane roughness correlations are very different for the 4 multilayer samples, which as a set show a strong correspondence in relative intensities and shapes to the set of substrate data. Thus, not only do the vertical roughness correlations in the multilayer appear highly correlated with the multilayer periodicity, but the in-plane roughness correlations in the multilayers appear nearly identical to those of the substrates. Even on the smoothest substrate, there is no indication of roughness in the multilayer which does not originate in the substrate. Taken together, these data suggest that roughness is these W/C multilayers is nearly perfectly correlated, resulting from conformal growth of an otherwise highly smooth multilayer to the roughness of the substrate. Other analyses reach similar conclusions [25], but also indicate that partially correlated roughness in larger d W/C multilayers plays a role at higher in-plane, and out-of-plane, spatial frequencies. From the trend of $\sigma$ with d we expect that partially correlated or uncorrelated roughness would play a larger role for multilayers with larger periods.

In summary, a simple analysis of peak reflectance data from many different x-ray multilayer systems prepared by numerous groups and having periods ranging from 9 to 130 Å reveal a common trend for the interface width $\sigma$ to increase in rough proportion to the period. In addition, there is a low $\sigma$ limit of

roughly 2 Å which is nearly reached by the smallest period samples. Specular and diffuse scattering measurements of uncoated and multilayer coated substrates indicate that the substrate contribution to $\sigma$ is dominant for high qualilty multilayers of very small period. The substrate contribution becomes relatively less important as the period increases, as the increase in $\sigma$ with period is accounted for by roughness and interdiffusion intrinsic to the layers themselves. This trend in effective $\sigma$ with d provides a realistic basis to calculate expected performance of high quality multilayers for various applications, and a standard by which to gauge the performance of new x-ray multilayer structures. Continued studies may yield improved understanding of the origins of and trends in structural imperfections in multilayer systems, and possibly to improvements in performance.

The author acknowledges D.G. Stearns for initiating the survey whose partial results were discussed here. The diffuse scattering data were collected at the Stanford Synchrotron Radiation Laboratory with assistance for T.D. Nguyen. This research was supported by the Director, Office of Energy Research, Office of Basic Energy Sciences, Materials Sciences Division of the U.S. Department of Energy under contract AC03-76SF00098.

References

1. E. Spiller, Appl. Phys. Lett. **20**, 365 (1972).

2. J.H. Underwood and T.W. Barbee, Jr., Appl. Opt. **20**, 3027 (1981).

3. B.L. Henke, J.Y. Uejio. H.T. Yamada and R.E. Tackaberry, Optical Engineering 25, 937 (1986).

4. E. Spiller, in *Physics, Fabrication, and Applications of Multilayered Structures*, P. Dhez and C. Weisbuch, eds. (Plenum, New York, 1988), p. 284.

5. M. Yamamoto and T. Namioka, Appl. Opt. **31**, 1622 (1992).

6. R.P. Haelbich, A. Segmuller, and E. Spiller, Appl.Phys. Lett. **34**, 184 (1979), and E. Spiller, in *Low Energy X-ray Diagnostics - 1981*, eds. D.T. Attwood and B.L. Henke, AIP Conf. Proc. 75, p. 124.

7. T.W. Barbee, in *Low Energy X-ray Diagnostics - 1981*, eds. D.T. Attwood and B.L. Henke, AIP Conf. Proc. 75, p. 131.

8. D.E. Savage, J. Kleiner, N. Schimke, Y.H. Phang, T. Jankowsky, J. Jacobs, R. Dariotis, and M.G. Lagally, J. Appl. Phys. 69, 1411 (1991).

9. J.B. Kortright, J. Appl. Phys. **70**, 3620 (1991).

10. D.G. Stearns, J. Appl. Phys. **72**, 4286 (1992).

11. Y.H. Phang, R. Kariotis, D.E. Savage, and M.G. Lagally, J. Appl. Phys. **72**, 4627 (1992).

12. A.P. Payne and B.M. Clemens, Phys. Rev. B **47**, 2289 (1993), and *ibid* p. 16068 (1993).

13. V. Holy and T. Baumbach, Phys. Rev. B **49**, 10668 (1994).

14. D.G. Stearns, J. Appl. Phys. 65, 491 (1989).

15. A.K. Petford-Long, M.B. Stearns, C.H. Chang, S.R. Nutt, D.G. Stearns, N.M. Ceglio, and A.M. Hawryluk, J. Appl. Phys. 61, 1422 (1987).

16. R.S. Rosen, D.G. Stearns, M.A. Viliardos, M.E. Kassner, S.P. Vernon and Y. Cheng, Appl. Opt. 32, 6975 (1992).

17. J.B. Kortright, S. Joksch, and E. Ziegler, J. Appl. Phys. 69, 168 (1991).

18. H. Takenaka, T. Kawamura, Y. Ishii, T. Haga, and H. Kinoshita, in *OSA Proceedings on Extreme Ultraviolet Lithography, 1994, Vol. 23* (Optical Society of America, 1995) eds. F. Zernike and D.T Attwood, p. 26.

19. The survey was conducted at the Physics of X-Ray Multilayer Topical Conference of the Optical Society of America, 14-17 March 1994, Jackson, Wyoming, chaired by J.B. Kortright, D.G. Stearns and D.L. Windt, from whom copies of survey results can be obtained.

20. K.M. Skulina, C.S. Alford, R.M. Bionta, D.M. Makowiecki, E.M. Gullikson, R. Soufli, J.B. Kortright and J.B. Underwood, Appl. Optics 34, 3727 (1995).

21. J.H. Underwood, E.M. Gullikson, and K. Nguyen, Appl. Opt. 32, 6985 (1993).

22. B.L. Henke, E.M. Gullikson, and J.C. Davis, At. Data Nucl. Data Tables 54, 181 (1993).

23. J.B. Kortright and J.Denlinger, Mat. Res. Soc. Symp. Proc. Vol. 103, 95 (1988).

24. G.M. Lamble, S.M. Heald, D.E. Sayers, E. Ziegler, and P.J. Vicarro, J. Appl. Phys. 65, 4250 (1989).

25. Y.H. Phang, D.E. Savage, R. Kariotis, and M.G. Lagally, J. Appl. Phys. 74, 3181 (1993).

## Figure Captions

**Figure 1.** (a) shows results of a survey of near-normal incidence peak reflectance results as a function of photon energy. Vertical lines indicate core atomic absorption edges for certain elements below which they are near optimal weak scatterers for inclusion in x-ray multilayers. Different symbols indicate the weak scatterer in the multilayer, and each symbol may result from multilayers with one or more strong scatterer. Strong scatterers with C are W, Ru, Cr, Ge, NiCr, and $Cr_2C_3$. Strong scatterers with Si are Mo, and Ru. Strong scatterers with $B_4C$ are Ru, Mo, Pd. Strong scatterers with B are Ag, Mo, Pd. ReW, Si and Ti. The strong scatterer with Be is Mo, with Al is Zr, and with Y is Mo. (b) shows the ratio of measured to ideal calculated reflectance for multilayers corresponding to a representative set of multilayers in (a).

**Figure 2.** Effective $\sigma$ values needed to match measured to calculated ideal peak reflectance are plotted vs. the multilayer period. Data points from the near-normal incidence survey are included, as are data from several $W/B_4C$ multilayers measured at grazing incidence with Cu K$\alpha$ radiation to extend the data set to smaller d. $\sigma$ decreases with d, and appears to reach a lower limit of about 2 Å. A linear fit is shown.

**Figure 3.** (a) shows the specular reflectance of a set of 4 fused silica flat substrates polished to different levels of smoothness. Substrate 1 is smoothest, 4 roughest. Solid lines are fits to the data. (b) shows a specular scan and a parallel, off-specular scan from a W/C multilayer deposited onto a substrate identically polished as the sample 1 in (a). The diffuse Bragg peaks are just as strong as the specular Bragg peak, indicating that the roughness has the same vertical correlations as the multilayer itself.

**Figure 4.** (a) shows rocking scans taken at $2\theta = 2.00°$ from the 4 different substrates showing different specular and diffuse intensities. (b) shows the same rocking scans from the W/C multilayer on the 4 different substrates. The diffuse intensity from the multilayers shows very similar in-plane roughness correlations as the substrates. Lines connect data points.

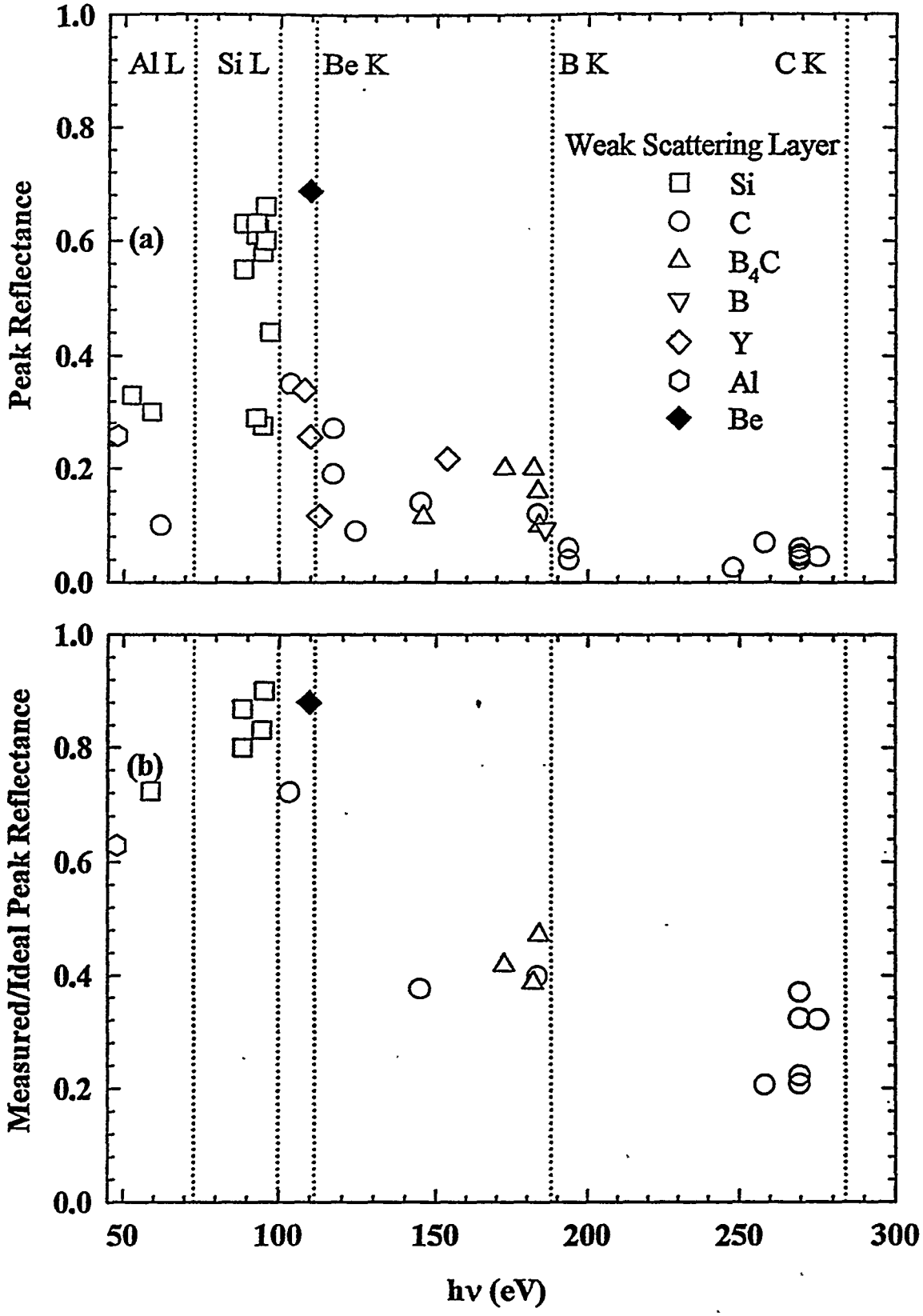
Al L
Si L
Be K
B K
C K
Weak Scattering Layer
Si
C
$B_4C$
B
Y
Al
Be
(a)
(b)
Peak Reflectance
Measured/Ideal Peak Reflectance
hν (eV)
1.0
0.8
0.6
0.4
0.2
0.0
50
100
150
200
250
300

**Figure 1**

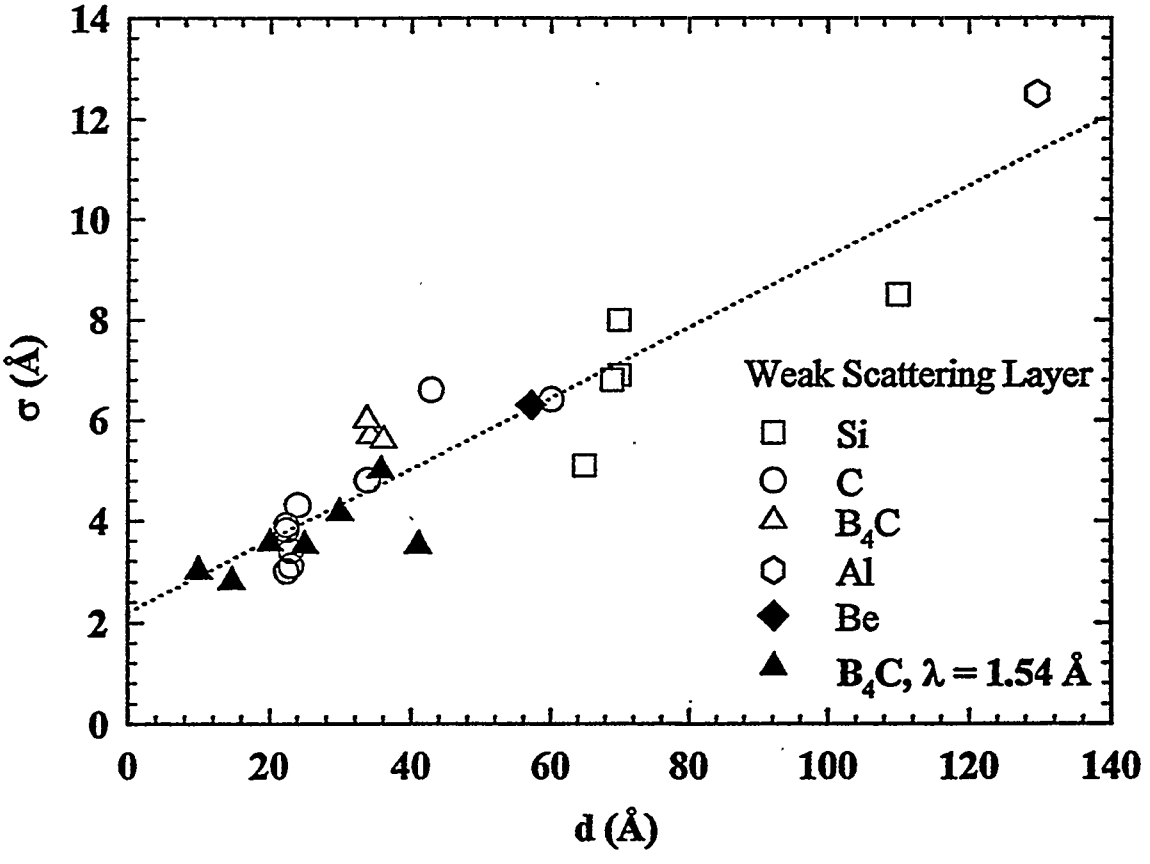
14
12
10
8
6
4
2
0
σ (Å)
0
20
40
60
80
100
120
140
d (Å)
Weak Scattering Layer
Si
C
B4C
Al
Be
B4C, λ = 1.54 Å

**Figure 2**

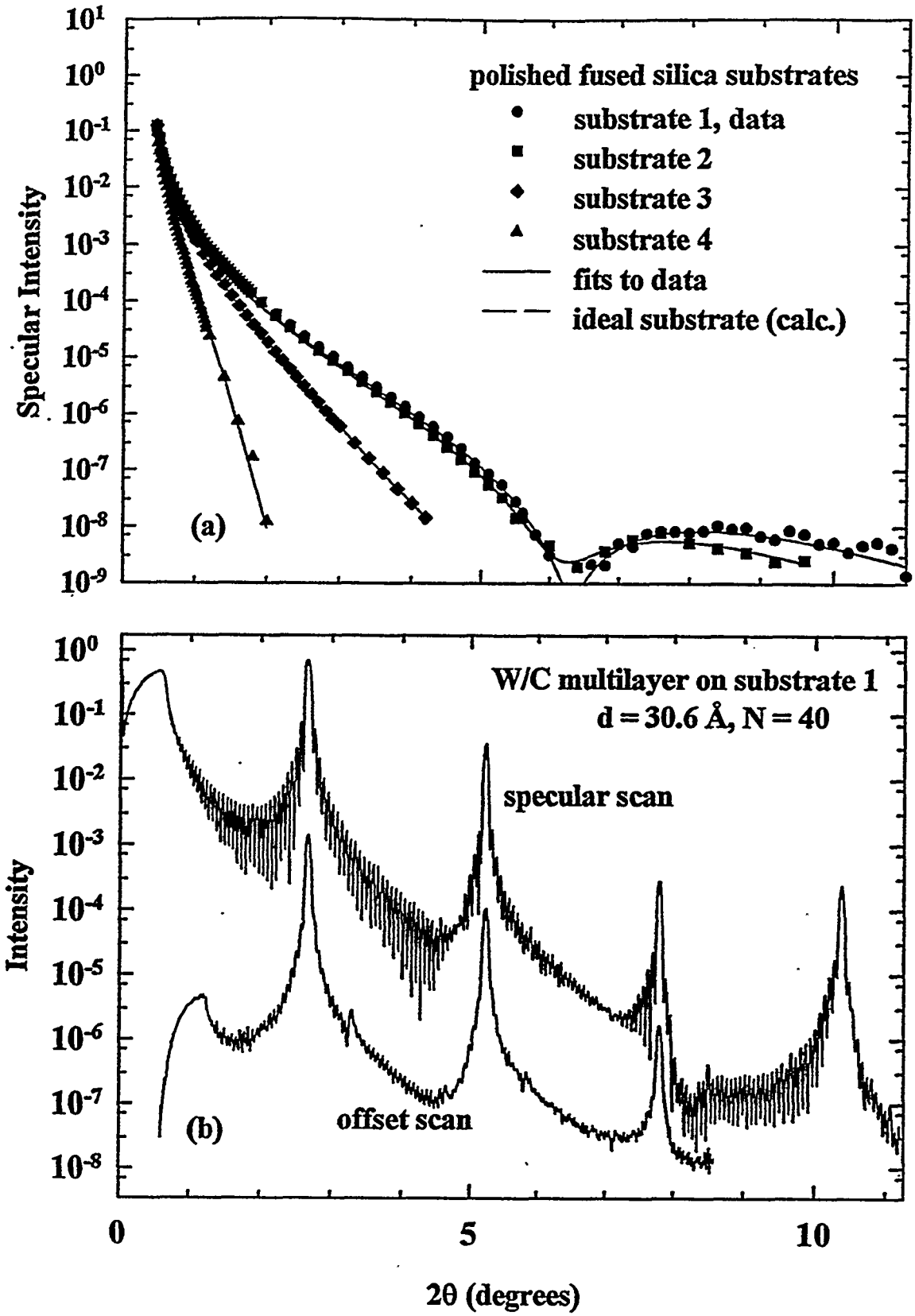
polished fused silica substrates
substrate 1, data
substrate 2
substrate 3
substrate 4
fits to data
ideal substrate (calc.)
Specular Intensity
(a)
W/C multilayer on substrate 1
d = 30.6 Å, N = 40
specular scan
offset scan
(b)
Intensity
2θ (degrees)

Figure 3

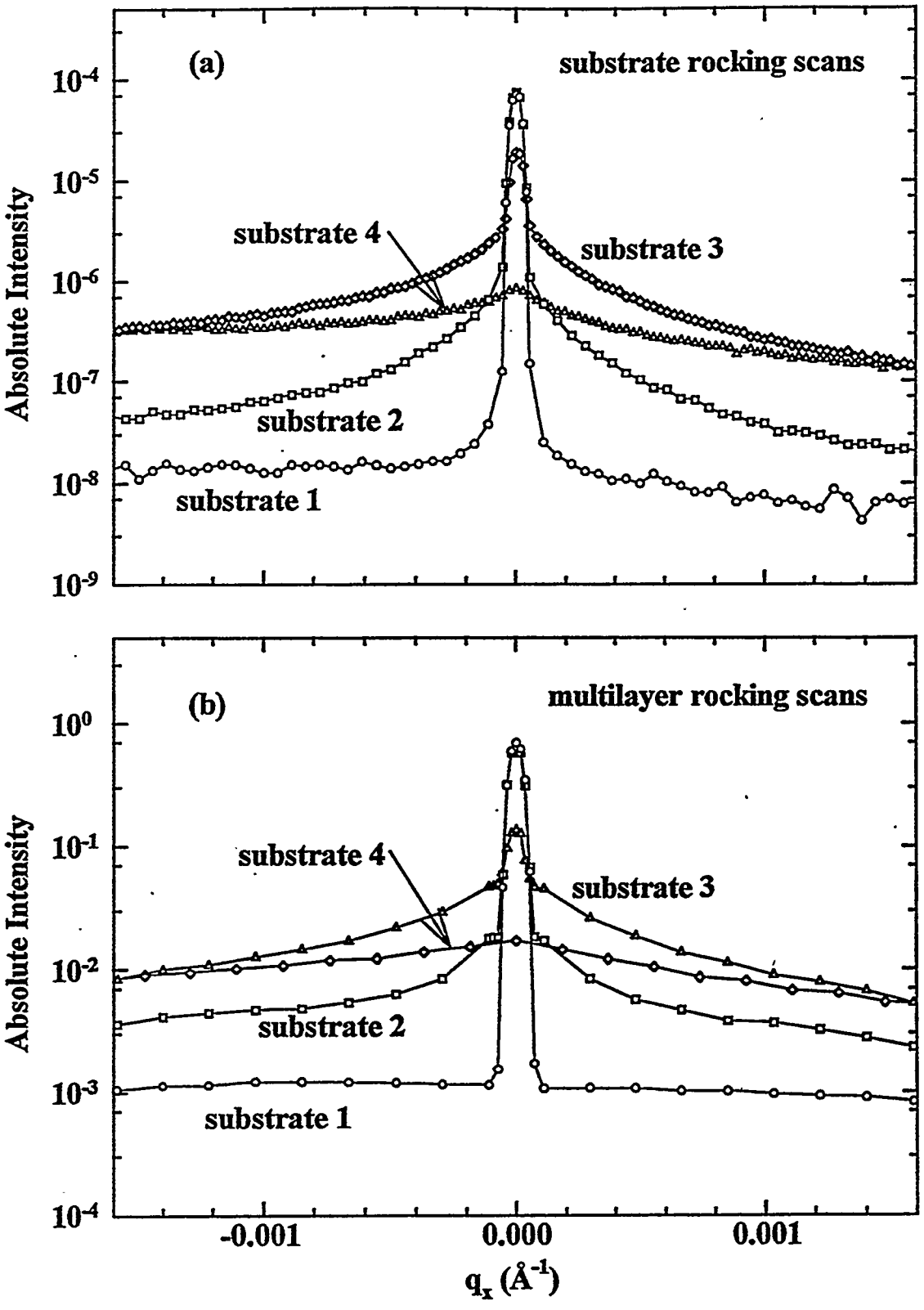
(a)
substrate rocking scans
Absolute Intensity
$10^{-4}$
$10^{-5}$
$10^{-6}$
$10^{-7}$
$10^{-8}$
$10^{-9}$
substrate 4
substrate 3
substrate 2
substrate 1
(b)
multilayer rocking scans
Absolute Intensity
$10^{0}$
$10^{-1}$
$10^{-2}$
$10^{-3}$
$10^{-4}$
substrate 4
substrate 3
substrate 2
substrate 1
-0.001
0.000
0.001
$q_x$ (Å$^{-1}$)

Figure 4

LAWRENCE BERKELEY NATIONAL LABORATORY
UNIVERSITY OF CALIFORNIA
TECHNICAL & ELECTRONIC INFORMATION DEPARTMENT
BERKELEY, CALIFORNIA 94720